Electrochimica Acta, Vol. 38, No. 12, pp. 1661–1669, 1993
Printed in Great Britain.

0013–4686/93 $6.00 + 0.00

EFFECT OF SPUTTERED FILM OF PLATINUM ON LOW PLATINUM LOADING ELECTRODES ON ELECTRODE KINETICS OF OXYGEN REDUCTION IN PROTON EXCHANGE MEMBRANE FUEL CELLS

SANJEEV MUKERJEE, SUPRAMANIAM SRINIVASAN* and A. JOHN APPLEBY
Center for Electrochemical Systems and Hydrogen Research, Texas Engineering Experiment Station, Texas A&M University, College Station, TX 77843-3402, U.S.A.

(*Received* 5 *October* 1992; *in revised form* 1 *February* 1993)

Abstract—Localization of Pt electrocatalyst by sputter deposition of a thin film (500 Å) on the front surface of a fuel cell electrode containing a supported electrocatalyst (20% Pt/C, 0.4 mg cm^{-2} loading) has been known to exhibit higher fuel cell performance as compared to that on the electrode without the sputtered film. This study compares the electrode kinetic parameters, electrochemically active surface areas, activation energies and reaction orders for the oxygen reduction reaction (ORR) in the sputtered and unsputtered electrodes in proton exchange membrane fuel cells as functions of temperature and pressure. Comparison of the cell performance at 5 atm and 95°C indicates an almost 4 fold improvement in ORR activity at 0.9 V vs. *rhe* and a similar 3.6 fold improvement in the exchange current densities. The increment in the electrochemically active surface area was about two fold, thereby indicating that factors beyond a surface area increment were responsible for the observed activity enhancement in the ORR. Evaluation of ORR electrode kinetics as a function of temperature indicated a lower activation energy for ORR on the sputtered electrode, as compared to that on the unsputtered electrode. The reaction orders for ORR were, however, the same for both electrodes and were similar to previously obtained values at the Pt microelectrode/Nafion interface, thereby indicating no change in the rate determining step for ORR. This paper also presents the morphological characterization of the electrode/membrane interface using the SEM/EDAX technique, which clearly signifies the two types of Pt—unsupported and supported.

Key words: solid polymer electrolyte fuel cells, electrode kinetics, electrocatalysis, oxygen reduction.

INTRODUCTION

Attainment of high energy efficiencies and high power densities in PEMFCs with low platinum loading electrodes

The prospects of utilizing proton exchange membrane fuel cells (PEMFC) for space and terrestrial applications has become extremely attractive. The primary reasons are the ability to attain high power densities (~1.2 W cm^{-2}) at relatively low temperatures (55–95°C) and pressures of 5 atm. Such high power densities are attained via better utilization of Pt crystallites in the gas diffusion electrode structure. This has resulted in the reduction of Pt loading from 4 to 0.4 mg cm^{-2} (with only a small loss in performance)[1–5]; and the promise of further reduction in Pt loading to 0.1 mg cm^{-2} exists based on work in progress in our laboratory[6] as well as in two others[7, 8].

Most of these efforts towards higher Pt utilization has involved novel ways of Pt deposition on the electrode surface, such as the electrochemical ECC technique[8] and the localization of Pt near the front surface of the electrode by using thinner reaction layers as well as sputter deposition[5]. The motivation for the latter approach arose out of previous studies[5], indicating that at higher power densities the bulk of the current is generated close to the front surface of the electrode (see references cited in[5]). In addition to this, the technique of sputter deposition is well established (in semiconductor fabrication, mirror coatings *etc.*) and hence any resulting cost increment is expected to be more than compensated for due to higher Pt utilization and hence lower Pt requirements.

Previous studies on the localization of Pt *near the front surface to attain high energy efficiencies and high power densities*

In order to investigate the effect of thin active layers on the performance of PEMFCs, the effect of localization of Pt near the front surface was previously investigated at LANL (Los Alamos National Laboratory)[5]. For this purpose, electrodes containing 10, 20 and 40% Pt/C electrocatalysts with a platinum loading of 0.4 mg cm^{-2} were custom-made and evaluated in PEMFCs. The active layer, which contained the Pt/C electrocatalyst and Teflon (30%), was deposited on a Teflonised carbon-cloth substrate. Maintaining the constant Pt loading caused a progressive reduction in the thickness of the active layer, *ie* 100, 50 and 25 μm for the electrodes with 10, 20 and 40% Pt/C supported electrocatalysts. Reducing the reaction layer thickness showed signifi-

* Author to whom correspondence should be addressed.

cant improvements in performance in all the three potential (*ie* activation, ohmic and mass-transport controlled) regions (Fig. 1a). The improvement in performance was found to be more significant when the platinum content of the supported electrocatalyst was increased from 10 to 20% Pt/C than from 20 to 40% Pt/C. The interpretation of this result was that the Pt particle size is considerably greater in the 40% Pt/C than in the 20% Pt/C electrocatalyst. In all cases, the depth of penetration of the Nafion, by impregnation of solubilized Nafion and evaporation of the solvent, was nearly the same (10 μm) and thus the increase in performance of the single cell was attributed to the increase in electrochemically active surface area, as was confirmed by cyclic voltammetry. Further, by reducing the thickness of the active layer, mass-transport and ohmic overpotentials within the active layer were greatly reduced and thus higher power densities were attained in the cells with the electrodes containing the higher Pt/C content. This is because at the higher current densities the current distribution is such that the bulk of the current is generated close to the front surface.

A second approach of depositing a thin layer of Pt in the immediate vicinity of the electrode/membrane interface was also examined in the same investigation[5] as well as in a subsequent one[9]. Figure 1b shows the effect of a 50 nm sputtered film of Pt (0.05 mg cm^{-2}) on the electrodes containing 10, 20 and 40% Pt/C electrocatalyst[5]. Comparison of the 10% Pt/C, with and without the sputtered layer of Pt, indicates improvement in all three regions (activation, ohmic and mass-transport). Furthermore, in the investigations on the effect of a sputtered film of Pt on the electrodes with the three different types of Pt loading (with consequent reduction of the reaction layer thickness from 100–25 μm), the improvement in performance of the PEMFC, when using the electrodes with 20% Pt/C electrocatalyst was more than with 10% Pt/C. On the other hand, the performance of the electrode with the 40% Pt/C electrocatalyst and the sputter-deposited Pt film was not as good as that on the electrode with the 20% Pt/C electrocatalyst and the sputtered Pt film. This result was rationalized by the authors[5] on the basis that the 40% Pt/C electrocatalyst has a larger Pt crystallite size than the 20% Pt/C, which hence reduces the effective surface area of the Pt. According to a subsequent publication[10], transmission electron microscopic examination of the Pt/C electrocatalysts confirmed this explanation. These studies therefore indicate that an electrode with 20% Pt/C electrocatalyst and a 50 nm sputtered film on its front surface has the optimum configuration for a PEMFC. Furthermore, the lifetime studies on such an electrode[5] showed no loss in performance over a period of 1000 h.

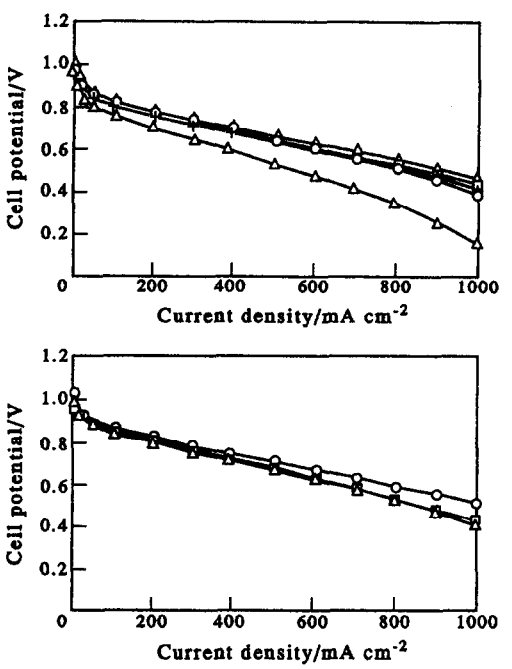

Fig. 1. (a) Effect of increase in wt% of Pt/C, in supported electrocatalyst (Protech). Operating conditions: 80°C and 3/5 atm; H_2/Air single cell performance. Pt loading (0.4 mg cm^{-2}): (△) 10; (○) 20; (□) 30; (◇) 40 wt% Pt/C electrodes[5]. (b) Effect of sputtered film deposited on different wt% Pt/C supported electrocatalyst (Prototech). Operating conditions 80°C and 3/5 atm; H_2/Air single cell performance: (△) 10; (○) 20; (□) 40 wt% Pt/C electrodes, with a 50 nm sputtered film and total Pt loading (0.45 mg cm^{-2})[5].

Scope of the present work

Based on the above mentioned results, which show an enhanced performance of PEMFCs with the reaction layers containing the sputtered film of Pt on the front surface, this work was carried out to examine the effects of the sputtered film of platinum, on the electrodes with 20% Pt/C electrocatalyst, on the electrode kinetics of oxygen reduction in PEMFCs. The present study on oxygen reduction at the sputtered and unsputtered electrodes in PEMFCs encompasses the determinations of: (i) electrochemically active surface areas of the electrodes, in order to ascertain the exchange current densities on the basis of the real surface area of the electrode; (ii) the electrode kinetic parameters as functions of temperature and pressure; and (iii) activation energies and reaction orders with respect to oxygen. Examination of the morphological characteristics of the two types of membrane and electrode assemblies were also made using SEM/EDAX techniques.

EXPERIMENTAL

Electrode structure and sputter-deposition of a thin film of Pt *on the front surface of an electrode*

The electrodes were custom-made by ETEK Inc. (Framingham, Massachusetts). The Teflonised carbon-cloth was used as a substrate. The active layer was composed of 30% Teflon and 70% of the supported electrocatalyst (20% Pt/C and a Pt loading of 0.4 mg cm^{-2}). The Pt film was sputtered on to the front surface of the E-TEK electrode using an Argon ion source, at the Los Alamos National Laboratory. The thickness of the deposited Pt layer

was 500 Å and the weight of the sputtered Pt amounted to 0.05 mg cm^{-2}. The sputtered layer of Pt obtained by such means was uniform and had Pt crystallites with an average size of 25–35 Å[10].

Preparation of the membrane and electrode assembly

As described in previous communications[1–5], the electrodes were impregnated with Nafion® solution (Nafion® 1100, 5% by weight dissolved in a mixture of lower alcohols, predominantly isopropyl alcohol, Aldrich Chemical Co.) using a brushing technique. This was followed by air-drying at 80°C and weighing; a Nafion loading of approximately 0.6 mg cm^{-2} is optimal. A Dow experimental membrane (XUS 13204.10, developmental fuel cell membrane) was first pretreated by heating in high purity water (Continental water purification system, Modulab type 1), followed by heating in 5% aqueous solution of H_2O_2 (J. T. Baker) for 1 h at about 70–80°C (to remove organic impurities). This was then heated in 0.5 M H_2SO_4 (J. T. Baker) at 70–80°C. Finally, the H_2SO_4 was removed by repeatedly treating with boiling water. The electrodes were then hot-pressed to the Dow membrane at a pressure of 70 atm and a temperature of 155°C for 90 s. This temperature was chosen because it is close to the glass-transition temperature of the Dow membrane.

Assembly of the single cell and its installation in the test station

The membrane and electrode (MEA) assembly was then incorporated in the single cell test fixtures. A schematic layout of the single cell test fixtures and the MEA assembly has been described elsewhere[11]. A platinised-platinum electrode, located in the anode compartment, served as the reversible hydrogen reference electrode. The single cell was then installed in the fuel cell test station. The test station is equipped for temperature control of the cell and reactant gases, humidification of the reactant gases and control of the gas flow rates using rotameters (Matheson). The total pressure of the gas was regulated using back-pressure regulators (Matheson). Electrical leads from the test station were connected to a programmable power supply (Hewlett–Packard model 6033A), which was interfaced with an IBM PS/2 personal computer for data acquisition, plotting and analysis.

Electrode kinetic and cyclic voltammetric experiments

Prior to the actual electrochemical performance evaluation, it was essential to attain the optimum environment, because when a single cell is assembled, the proton exchange membrane is in a dry state. It takes between 24 and 48 h for the MEA to achieve the optimum humidification conditions. For this purpose the cell was maintained at 50°C with the hydrogen and oxygen gases (1 atm) humidified at 60 and 55°C, respectively, while it was operated at a current density of 200 mA cm^{-2} for the first 24 h. After this period, the cell temperature was raised to 85°C the reactant gas pressure maintained at 5 atm and the water in the H_2 and O_2 humidification bottles to 95 and 90°C, respectively. It was then operated at a current density of 2 A cm^{-2}, for equilibration with the product water to attain optimal water absorption conditions by the proton exchange membrane. Thereafter the measurement of the cell and half cell potentials vs. current densities were made using the programmable power supply, interfaced with the computer. The investigated pressure and temperature ranges were 0–60 psig (1–5 atm.) and 40–80°C, respectively. All comparisons of the *iR*-corrected Tafel plots for oxygen reduction were made at 5 atm and 95°C with the oxygen and hydrogen humidified at 100 and 105°C. After the potential vs. current density measurements, hydrogen was passed through the counter electrode chamber and argon through the working electrode (cathode, oxygen electrode) compartment and the cyclic voltammograms (CVs) were then recorded on the electrodes to determine the electrochemically active surface areas. The potential range employed for recording the CVs was between 120 mV and 1 V vs. *rhe* at sweep rates ranging from 10–50 mV s^{-1}. Lower sweep rates were preferred in order to minimize the pseudo-transmission-line effects in the porous electrode. The electrochemically active surface area of the electrode was obtained from the charge required for hydrogen desorption from the Pt electrocatalyst.

Morphological characterization

The morphological characterization of the sputtered and unsputtered electrodes was conducted using SEM/EDAX techniques (JSM scanning microscope and by Tracor Northern Series 2 EDS with Z-max window for lighter elements). For this purpose the MEA assembly was embedded in a resin (Araldite) such that the cross-section involving the anode/membrane/cathode could be characterized. First, the scanning electron microscope image was observed at different points along the cross-section. This was followed by energy dispersive X-ray analysis (EDAX). The EDAX spectrum was recorded at several points along the cross-section by moving the sample under the electron-gun, using an $x - y$ manipulator.

RESULTS AND DISCUSSION

Electrochemically active surface area

The cyclic voltammograms for both the sputtered and unsputtered electrodes are shown in Fig. 2. In addition to the characteristic features for smooth Pt surfaces, the CV illustrates the following: (i) evidence for oxidation and reduction of organic species at potentials more positive than 0.85 V vs. *rhe*. This result is also supported by the relatively wide oxide–reduction peak, as compared to that on smooth Pt electrodes; and (ii) redox peaks probably corresponding to that of a quinone-hydroquinone couple. This is substantiated by previous work on fuel cell electrodes, using supported (Pt on Vulcan XC-72) electrocatalysts[3]. The electrochemically active surface areas were obtained from the CVs recorded at 10 mV s^{-1} on sputtered and unsputtered electrodes, *ie* by calculating the coloumbic charge for oxidation of the adsorbed atomic hydrogen (*ie* area

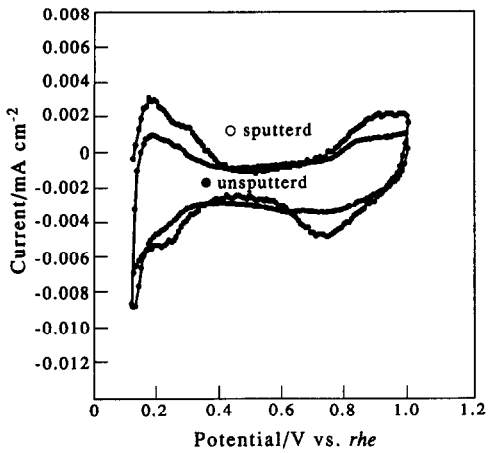

Fig. 2. Cyclic voltammograms for sputtered (0.45 mg cm^{-2} Pt) and unsputtered (0.40 mg cm^{-2} Pt) ETEK electrodes in proton exchange membrane fuel cells. Temperature 60°C, sweep rate 10 mV s^{-1}.

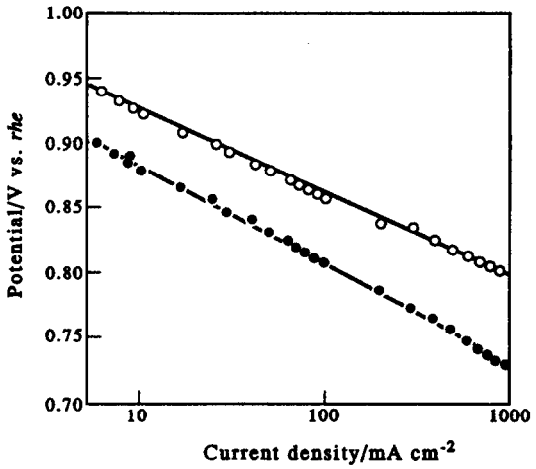

Fig. 3. *iR*-free Tafel plots for oxygen reduction on sputtered (0.45 mg cm^{-2}) and unsputtered (0.4 mg cm^{-2}) electrodes in proton exchange membrane fuel cells. Temperature: 95°C, pressure 5 atm, sputtered (○), unsputtered (●).

under the anodic peak minus double layer charge). The roughness factor was then calculated by assuming a coloumbic charge of 220 μC cm^{-2} for hydrogen adsorption or desorption on a smooth Pt surface. The calculated values of roughness factors are 49 for the unsputtered electrode and 88 for the sputtered electrode and hence the electrochemically active surface area for the electrode with a sputtered film is about 80% higher than that for the unsputtered one.

Electrode kinetic parameters at 5 atm and 95°C

Figure 3 shows that the half cell potential (E) vs. current density (i) data fit the equation:

$$E = E_0 - b \log i - Ri, \quad (1)$$

where

$$E_0 = E_r + b \log i_0. \quad (2)$$

In equations (1) and (2), i_0 is the exchange current density for oxygen reduction, b is the Tafel slope, E_r is the reversible potential for the oxygen electrode reaction and R represents the resistance (predominantly the ohmic resistance of the electrolyte) responsible for the linear variation of potential vs. current density plot. Equation (1) is valid up to the end of the linear region of the half cell potential vs. current density plot. At very high current densities, the departure of the E vs. i data from equation (1) is due to the onset of mass-transport limitations. The parameters E_0, b and R were evaluated by a non-linear least square fitting of equation (1) to the experimental data. Using the R values, the *iR*-corrected Tafel plots [$(E + iR$ vs. log $i)$] were constructed.

Comparison of the *iR*-free Tafel plots for oxygen reduction in the cells with the unsputtered and sputtered electrode (Fig. 3) at 95°C and 5 atm shows a decrease in the Tafel slope (57 vs. 62 mV dec^{-1}) and the ohmic resistance (0.125 vs. 0.091 ohm cm^{-2}) and an increase in the value of E_0 (960 vs. 998 mV) (Table 1). The values of exhange current densities were calculated after taking into consideration the effects of temperature and pressure on the reversible potential for the oxygen electrode reaction[11–13]. The exchange current densities show an increase from 1.5×10^{-4} A cm^{-2} for the unsputtered electrode to 5.4×10^{-4} A cm^{-2} for the sputtered one (approximately a 3.6 fold improvement). A similar increase should be expected for the rate of oxygen reduction at a potential of 0.9 V vs. *rhe*; as seen from

Table 1. Electrode kinetic parameters for oxygen reduction on low Pt loading electrodes (0.4 mg cm^{-2}), with and without a sputtered layer of Pt (0.05 mg cm^{-2}, 500 Å) on the front surface of the electrodes in proton exchange membrane fuel cells, operating at 95°C and 5 atm

Electrode	E_0 mV	b mV dec^{-1}	R ohm cm^2	i_0 mA cm^{-2} $\times 10^6$	Surface area* cm^2 cm^{-2}	i_0^* mA cm^{-2} $\times 10^4$	i_{900} mA cm^{-2}
Sputtered	998	62	0.091	6.36	88	5.4	25.4
unsputtered	960	57	0.125	3.06	49	1.5	6.6

i_{900} sputt./i_{900} unsputt.	i_0(sputt.)/i_0(unsputt.)	Surface area* (sputt./unsputt.)
3.9	3.6	1.8

* Electrochemically active surface area, i_0^* based on this area.

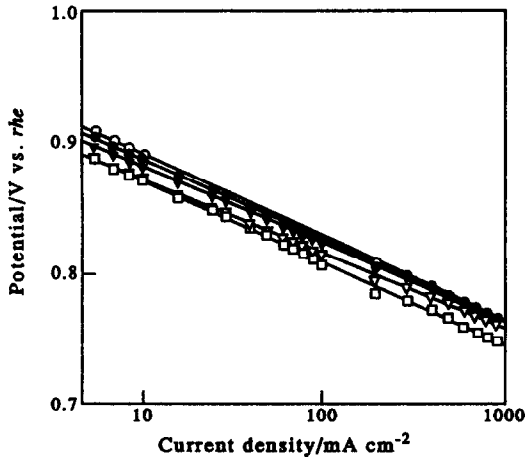

Fig. 4. *iR*-free Tafel plots for oxygen reduction on low Pt loading (0.4 mg cm^{-2}) electrodes, with a sputtered Pt layer (0.05 mg cm^{-2}), 500 Å, in proton exchange membrane fuel cells as a function of temperature: 40°C (□); 50°C (▽); 60°C (▲); 70°C (●); and 80°C (○).

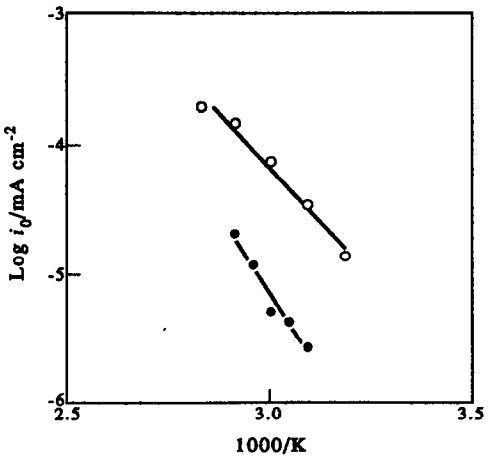

Fig. 6. Arrhenius plot for oxygen reduction on low Pt loading electrodes (0.4 mg cm^{-2}), with and without a layer of sputtered Pt (0.05 mg cm^{-2}, 500 Å). Sputtered (○), unsputtered (●).

Table 1, the increase in this rate is by a factor of 4. The fact that the observed improvement is not just due to an increased electrochemically active surface area is apparent from the values of the exchange current densities based on the true surface areas (see Table 1).

Effect of temperature on electrode kinetic parameters

Figures 4 and 5 shows the *iR*-corrected Tafel plots at several temperatures for the carbon supported (E-TEK) electrodes (0.4 mg cm^{-2}) with and without a layer of sputtered Pt (0.05 mg cm^{-2}, 500 Å) deposited on the front surface. These plots and Table 2 show that there is only a minor variation in Tafel slope with temperature. This is also the case for the unsputtered electrodes. However, the variation of E_0 with temperature is considerably higher for the unsputtered electrodes than for the sputtered electrodes. This is also apparent from the values of exchange current densities at various temperatures for sputtered and for unsputtered electrodes (Table 2). The plots of log i_0 vs. $1/T$ for the sputtered and unsputtered electrodes (Fig. 6) hence reveal lower activation energies for ORR on the sputtered electrode than on the unsputtered electrode (63 kJ mole^{-1} for sputtered and 82.5 kJ mole^{-1} for unsputtered). Therefore, improvement in the performance of ORR on the sputtered electrode is not only due to an enhancement of the electrochemically active surface area but may also be due to a lower activation energy for ORR.

Effect of pressure on electrode kinetic parameters

Figures 7 and 8 shows the *iR*-corrected Tafel plots at several pressures for the carbon supported ETEK electrodes (0.4 mg cm^{-2}), with and without a layer of

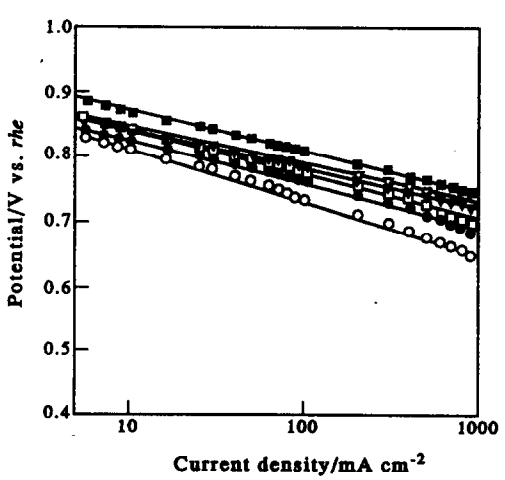

Fig. 5. *iR*-free Tafel plots for oxygen reduction on low Pt loading (0.4 mg cm^{-2}) electrodes, in proton exchange membrane fuel cells as a function of temperature: 40°C (○); 50°C (●); 55°C (□); 60°C (▼); 65°C (▽); 70°C (■).

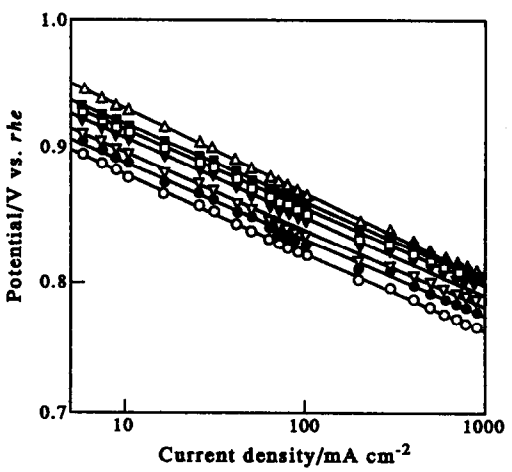

Fig. 7. *iR*-free Tafel plots for oxygen reduction on low Pt loading electrodes (0.4 mg cm^{-2}), with a sputtered Pt layer (0.05 mg cm^{-2}, 500 Å) in proton exchange membrane fuel cells at 70°C as a function of pressure: 0.67 (○); 1.57 (●); 2.05 (▽); 2.72 (▼); 3.41 (□); and 4.80 atm (△).

Table 2. Electrode kinetic parameters for oxygen reduction as a function of temperature on the sputtered and unsputtered electrodes in proton exchange membrane fuel cells at 1 atm

Sputtered electrode: cell pressure = 1 atm.

Temp. °C	E_r mV	E_0 mV	b mV dec^{-1}	R ohms cm^2	i_0 mA cm^{-2} $\times 10^5$	i_{850} mA cm^{-2}
40	1210	930	57.2	0.13	1.3	20.24
50	1204	940	58.9	0.12	3.3	40.25
60	1198	935	63.5	0.12	7.2	70
70	1190	950	62.5	0.11	14.1	93
80	1182	951	62.0	0.10	18.9	105

Unsputtered electrode

Temp. °C	E_r mV	E_0 mV	b mV dec^{-1}	R ohms cm^2	i_0 mA cm^{-2} $\times 10^5$	i_{850} mA cm^{-2}
40	1210	879	59.1	0.19	0.2	2.8
50	1204	880	58.2	0.17	0.3	6.9
55	1200	888	57.6	0.14	0.4	9.9
60	1198	910	54.2	0.13	0.5	13.42
65	1193	930	52.6	0.12	1.1	20.46
70	1190	946	52.0	0.12	2.0	48.44

sputtered Pt (0.05 mg cm^{-2}, 500 Å) deposited on the front surface. These Tafel plots are almost parallel for both the sputtered and unsputtered electrodes. From the values of the Tafel slopes (Table 3), it is apparent that both types of electrodes exhibit similar variation in Tafel slopes ($\Delta b = \sim 6$ mV decade^{-1}) with pressure in the range of 1–5 atm. Such a low increase in Tafel slope with pressure, has been previously reported[11]. Increases were also noted in the values of E_0 when the pressure was increased from 1 to 5 atm (for the sputtered electrodes $\Delta E_0 =$ 64 mV and for unsputtered electrodes $\Delta E_0 = 57$ mV). The exchange current densities in Table 3 were calculated after taking into account the pressure and temperature dependence of E_r[11–13] and the correction for the vapor pressure of water[11]. Plots of log exchange current density vs. log oxygen pressure (after correction for the vapor pressure of water) are shown in Fig. 9. These plots have nearly identical slopes, close to unity, indicating that the reaction order for both sputtered and unsputtered electrodes with respect to oxygen reduction is close to unity. For a nth order reaction, it can be shown that at any current density i, the equation

$$(\delta E/\delta \log P_0)_i = b \times n\mathrm{O}_2 \qquad (3)$$

is valid. In this equation, b is the Tafel slope, E_0 is the potential at 1 mA cm^{-2} and P_0 is the corrected pressure. The slope of the E_0 vs. log P_0 (Fig. 10) and use of equation (3) also indicates a reaction order of unity for both types of electrodes. This value of the reaction order for both sputtered and unsputtered electrodes suggests the same rate-determining step

$$\mathrm{M{-}{-}{-}O_2 + H^+ + e^- \rightarrow M - O_2H} \qquad (4)$$

in both cases where M is a surface Pt crystallite site.

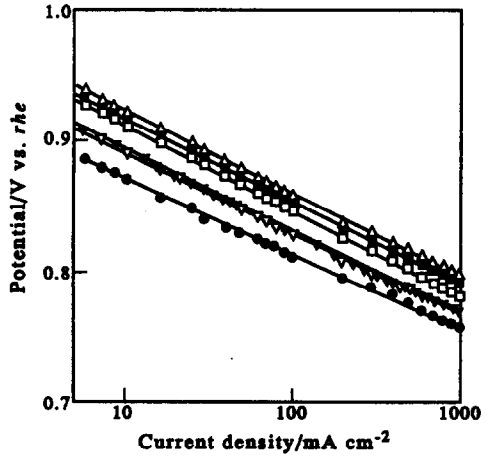

Fig. 8. iR-free Tafel slopes for oxygen reduction on low Pt loading electrodes (0.4 mg cm^{-2}) in proton exchange membrane fuel cells at 70°C as a function of pressure: 0.67 (○); 2.05 (▼); 2.72 (▽); 3.41 (□); 4.10 (■); and 4.80 atm (△).

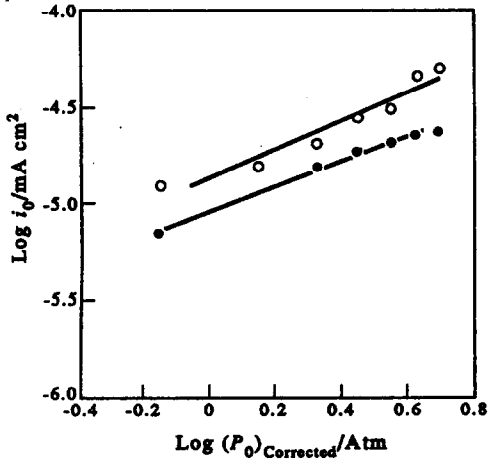

Fig. 9. Plot of exchange current density vs. pressure for oxygen reduction on low platinum loading electrode (0.4 mg cm^{-2}), with and without a sputtered layer (0.05 mg cm^{-2} Pt, 500 Å), in proton exchange membrane fuel cells. Temperature = 70°C, sputtered (○), unsputtered (●).

Table 3. Electrode kinetic parameters for oxygen reduction in proton exchange membrane fuel cells as a function of pressure for the sputtered and unsputtered electrodes at 70°C. Pt loading 0.45 mg cm^{-2} for sputtered electrodes and 0.40 mg cm^{-2} for unsputtered electrodes

Sputtered electrode

Oxygen pressure (atm)	E_r mV	E_0 mV	b mV dec^{-1}	R ohms cm^2	i_0 mA cm^{-2} $\times 10^5$	i_{900} mA cm^{-2}
0.67	1204	948	52.4	0.113	1.25	5.8
1.57	1214	944	56.4	0.109	1.62	7.4
2.05	1222	952	57.7	0.109	2.13	8.9
2.72	1235	964	56.9	0.110	2.95	10.4
3.41	1244	979	58.0	0.099	3.30	14.0
4.10	1253	990	60.1	0.092	4.90	17.2
4.80	1260	1012	58.1	0.096	5.37	22.1

Unsputtered electrode

Oxygen pressure (atm)	E_r mV	E_0 mV	b mV dec^{-1}	R ohms cm^2	i_0 mA cm^{-2} $\times 10^5$	i_{900} mA cm^{-2}
0.67	1204	938	51	0.132	0.71	1.0
2.05	1222	942	58.3	0.124	1.02	2.9
2.72	1235	960	58.4	0.124	1.99	3.3
3.41	1244	972	58.6	0.121	2.24	3.9
4.10	1253	990	57.0	0.110	2.46	4.4
4.80	1260	995	57.7	0.111	2.57	5.0

Correlation of electrode kinetic parameters with morphological characteristics of the electrode/membrane interface

Figure 11a and b shows the EDAX spectrum for various elements in the Dow membrane/cathode (oxygen electrode) interface (0.4 mg cm^{-2} Pt loading, with and without a layer of sputtered Pt, Pt content in the sputtered layer 0.05 mg cm^{-2} on the front surface). The most distinctive features of these spectra can be recognized by comparing the peaks for carbon and Pt in the unsputtered electrode; there is clear evidence of a supported electrocatalyst structure close to the interface with the Dow membrane, as indicated by the presence of peaks for both C and Pt. In the case of the sputtered electrode, there is a primary peak for Pt and evidence for only very minute amounts of carbon. The spectra confirms the predominance of Pt crystallites on the front surface of the electrode. Besides carbon and Pt, monitoring the fluorine at the sputtered electrode/membrane interface shows the lack of a Teflonized Pt structure on the sputtered electrode near the interface with the Dow membrane.

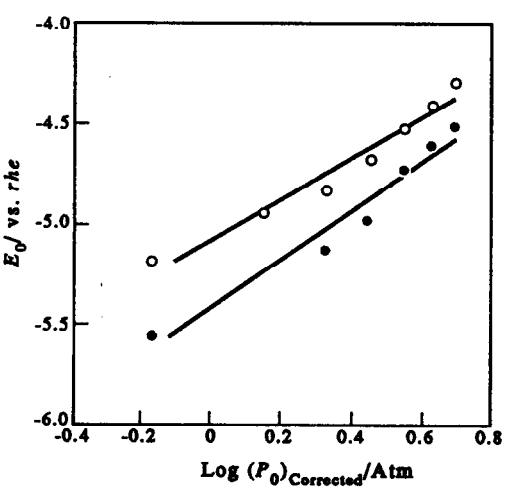

Fig. 10. Plot of E_0 vs. log P_0 for oxygen reduction at low platinum loading electrode (0.4 mg cm^{-2}), with and without a sputtered layer (0.05 mg cm^{-2} Pt, 500 Å), in proton exchange membrane fuel cells. Temperature = 70°C, sputtered (○), unsputtered (●).

CONCLUSIONS

This investigation compares the oxygen reduction kinetic parameters at several temperatures and pressures on fuel cell electrodes containing low Pt loading (0.4 mg cm^{-2}) electrodes, with and without a sputtered Pt film (0.05 mg cm^{-2}). The localization of Pt on the front surface of the electrode by sputter-deposition of a thin Pt film, clearly demonstrates improved ORR kinetics, which manifests itself in terms of a 4 fold improvement of current density at 0.9 V vs. *rhe* and of the exchange current density in a PEMFC at 95°C and 5 atm. Taking into consideration that the electrochemically-active surface area of the sputtered electrode is twice that of the unsputtered one, the exchange current density for oxygen reduction based on the true surface area is higher by a factor of two for the sputtered electrode (Table 4). The activation energy for ORR is lower for the electrode with the sputtered film. The measurement of electrode kinetic parameters as a function of pressure reveals that both the sputtered and unsputtered electrodes have nearly the same reaction orders. This indicated that both the sputtered as well as unsputtered electrodes have the same rate determining step. Comparison of the exchange current

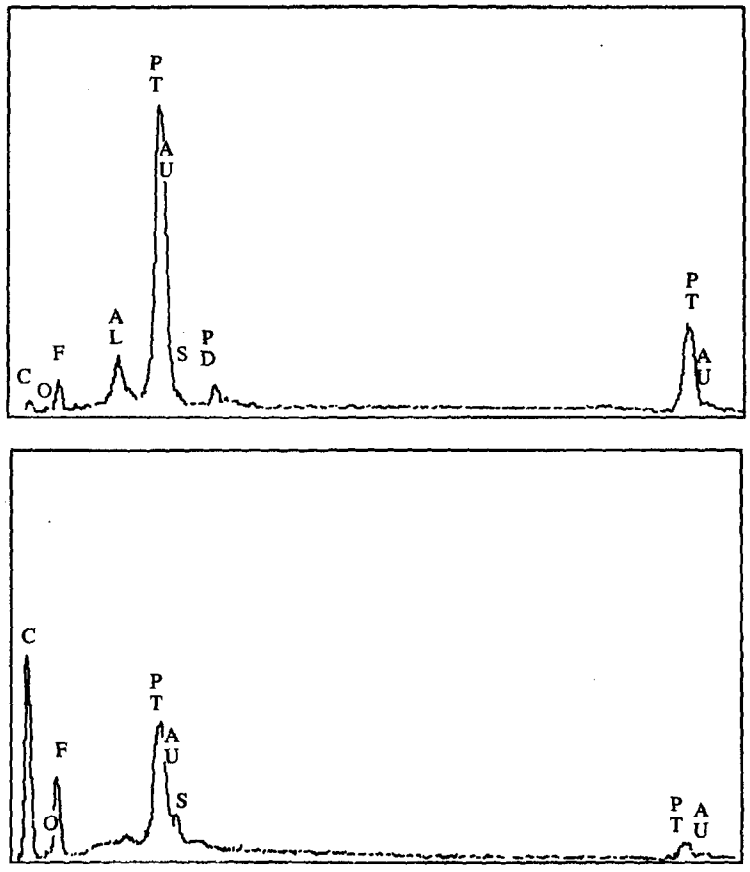

Fig. 11. (a) EDAX spectrum of the sputtered electrode/Dow membrane interface. (b) EDAX spectrum of the unsputtered electrode/Dow membrane interface.

Table 4. Electrode kinetic parameters, activation energies and reaction orders for oxygen reduction on low Pt loading electrodes with and without a sputtered layer (0.05 mg cm^{-2} 500 Å) of Pt in proton exchange membrane fuel cells and at a Pt microelectrode/Nafion interface

Electrode	Tafel slope* mV dec^{-1}	i_0* mA cm^{-2} $\times 10^4$	Surface area† cm^2 cm^2	i_0‡ mA cm^{-2} $\times 10^6$	Activation energy kJ mole^{-1}	Reaction order
Sputtered	57	5.4	88	6.12	63	0.99
Unsputtered	62	1.5	49	3.06	82	0.96
Microelectrode§	65	0.26	9.2	2.83	77	1.0

* Cell operating conditions: 95°C and 5 atm.
† Electrochemically active surface area.
‡ Exchange current density normalized with respect to the electrochemically active surface area, $T = 95$°C, $P = 5$ atm.
§ Data from[11].

densities normalized for the electrochemically active surface area for the sputtered, unsputtered as well as the microelectrode (Table 4) shows very close values for the microelectrode and the unsputtered electrode, the sputtered electrode, however, exhibits a higher value which could be accounted for on the basis of a different morphological environment in the immediate vicinity of the electrode/membrane interface. The localization of platinum near the front surface of the electrode without any Teflonized structure has therefore a beneficial effect on the ORR activity.

Acknowledgements—This work was carried out under the auspices of the National Aeronautical and Space Administration–Johnson Space Center (Regional University Grant # NAG 9-533). The authors wish to thank Dr A. Cesar Ferreira and Mr Omourtag A. Velev for helpful discussions and suggestions.

REFERENCES

1. I. D. Raistrick, in *Proceedings of The Symposium on Diaphragms, Separators and Ion Exchange Membranes*, p. 172. The Electrochemical Society (1986).

2. I. D. Raistrick, U.S. Patent. 4,876,115 (1989).
3. S. Srinivasan, E. A. Ticianelli, C. R. Derouin and A. Redondo, *J. Power Sources* **22,** 359 (1988).
4. E. A. Ticianelli, C. R. Derouin, A. Redondo and S. Srinivasan, *J. electrochem. Soc.* **135,** 2209 (1988).
5. E. A. Ticianelli, C. R. Derouin and S. Srinivasan, *J. electroanal. Chem.* **251,** 275 (1988).
6. A. C. Ferreira, S. Srinivasan and A. J. Appleby, *Extended Abstracts of the 181st Meeting of the Electrochemical Society*, **92-1,** 7 (1992).
7. M. S. Wilson and S. Gottesfeld, *J. appl. Electrochem.* **21,** 1572 (1991).
8. E. J. Taylor, E. B. Anderson and N. R. K. Vilambi, *J. electrochem. Soc.* **139,** L45–46 (1992).
9. S. Srinivasan, D. J. Maubo, H. Koch, M. A. Enayetullah and A. J. Appleby, *J. Power Sources* **29,** 367 (1990).
10. J. G. Beery, E. A. Ticianelli and S. Srinivasan, *J. appl. Electrochem.* **21,** 597 (1991).
11. A. Parthasarthy, S. Srinivasan, A. J. Appleby and C. R. Martin, *J. electronal. Chem.* **339,** 101 (1992).
12. G. N. Lewis and M. Randall, *International Critical Tables*, Vol. 7, p. 232. McGraw Hill, New York (1930).
13. K. Kinoshita, F. R. McLarnon and E. J. Cairns, in *Fuel Cell Handbook*, DOE contract No. DE-ACO3-765F00098, p. 10, May (1988).